Progress In Electromagnetics Research M, Vol. 48, 77–85, 2016

A Dual-Polarized Switchable Active Frequency Selective Surface for LTE-D Band

Chenchen Yang, Huangyan Li, Qunsheng Cao*, and Yi Wang

Abstract—A dual-polarized active frequency selective surface (AFSS) with switch function at LTE-D band is proposed in this paper. Double coupled metallic meandered structures on a one-layer substrate loaded PIN diodes are designed carefully to realize the band-pass characteristic at 2.6 GHz when PINs are OFF and the rejection characteristic when PINs are ON. The proposed model requires no additional biasing lines, and the amount of PINs is acceptable and affordable, which contribute to the simplicity and practicality of this AFSS in real applications. A simple equivalent circuit model (ECM) is given to better understand the design. Through full-wave simulation results, the polarization characteristics under TE and TM are almost the same, and the angle-stability stays well till 45°. For necessary verification, one finite FSS prototype was fabricated, which was changed to one switchable AFSS by welding PINs and external feeder lines. The measured results of transmission coefficient are obtained by free space test method in the microwave anechoic chamber and agree well with the simulated ones.

1. INTRODUCTION

Electromagnetic pollution is a new form of pollution, and it is estimated that man-made electromagnetic radiation has increased millions of times in last few decades [1]. Long Term Evolution (LTE) as the mainstream standard of the 4th generation mobile communication has been widely used recently. Shielding to protect some sensitive electronic devices is very necessary because radiation from LTE sources may produce interference that can cause equipment malfunction.

Frequency Selective Surfaces (FSSs) are spatial electromagnetic (EM) filters constituted by two-dimensional periodic metallic patch or aperture to transmit desired frequency signals and reflect the undesired. Over past years, FSSs have been extensively used in a variety of applications such as designing stealth radomes for aircrafts, dichroic reflector antennas, EM shielding for EMC and RCS reduction by EM absorbers to name a few [2]. A passive FSS has some limits because it offers no flexibility once fabricated, whereas an Active FSS (AFSS) allows the potentiality of control by changing the behavior of the surface [3–14]. As far as we know, the reconfigurable AFSSs can be divided into two main categories. One is switchable AFSSs which can switch frequency response between transmission and reflection at a specific frequency [3–8], and the other is tunable AFSSs whose frequency response can be shifted and tuned within a certain range [9–14]. The square-loop switchable AFSSs were realized by loading PINs inside elements or adjacent space, which were the first proposed AFSS as far as we know [3, 4]. Similarly, Mias used reactive components and varactor diodes inside square-loop FSS to achieve the tunable AFSS [9, 10]. However, all above reconfigurable AFSS designs are polarization-dependent, not suitable for real applications. To achieve polarization-independent performance, a new back prove-fed method through vias inside substrate was invented, which still needs a biasing network in bottom layer and not easy to be manufactured [5, 6]. Moreover, some scholars combined the structures and

Received 20 January 2016, Accepted 14 April 2016, Scheduled 4 May 2016
* Corresponding author: Qunsheng Cao (qunsheng@nuaa.edu.cn).
The authors are with the College of Electronic and Information Engineering, Nanjing University of Aeronautics and Astronautics, Nanjing 211106, China.

feeder lines together and adopted reasonable topology to avoid extra biasing network for easy design and better performance [7, 8, 11–14]. In [7], the popular ring element FSS was used to realize good performance in terms of all polarization affected and good angular stability by PINs and inductors. In [14], a novel band-stop active FSS capable of modifying their response for different polarizations was proposed. However, these designs need a large amount of active components (one unit structure needs at least four components averagely). In summary, the design of reasonable structure and integrated feeder with appropriate amount of PINs supporting TE and TM polarizations simultaneously is very attractive to us.

In this paper, a dual-polarized switchable AFSS is presented, which is totally transparent for 2.6 GHz LTE-D band (2.575–2.615 GHz) signals at the OFF state while shields those signals at the ON state. The resonant elements themselves act as feeder lines directly to reduce design complexity and negative impact of biasing network. The full-wave simulation results of the proposed structure are obtained by CST Microwave Studio and show good stability with respect to different polarizations and incident angles. Furthermore, a prototype AFSS is fabricated and measured in a microwave anechoic chamber. The measured results agree well with the simulated ones. This design shows potential applications at intelligent EM compatibility (EMC), smart stealth radome, EM architecture of buildings (EAoB), etc.

2. DESIGN PRINCIPLE AND GUIDELINE

2.1. Dual-Polarized Passive FSS Model

The dual-polarized passive FSS (PFSS) is shown in Figure 1, consisting of a one-layer F4B-2 substrate, with relative permittivity 2.65, loss tangent 0.001 and thickness 1 mm, and two-layer metallic meander line structures with orthogonal arrangement direction on the both sides of this substrate.

The dimensions of the unit cell through careful design are $U = 60$ mm, $L = 17.6$ mm, $w = 2.6$ mm, and $g = 1.5$ mm. The periodic boundary condition (PBC) is used in simulation software to get the S-parameters in Figure 1. This PFSS shows good transmission coefficient at 2.6 GHz with only insert loss 0.14 dB and -3 dB bandwidth 1.07 GHz under normal incidence. Besides, the performances for both TE and TM polarizations are identical, which means that this PFSS is quite dual-polarized.

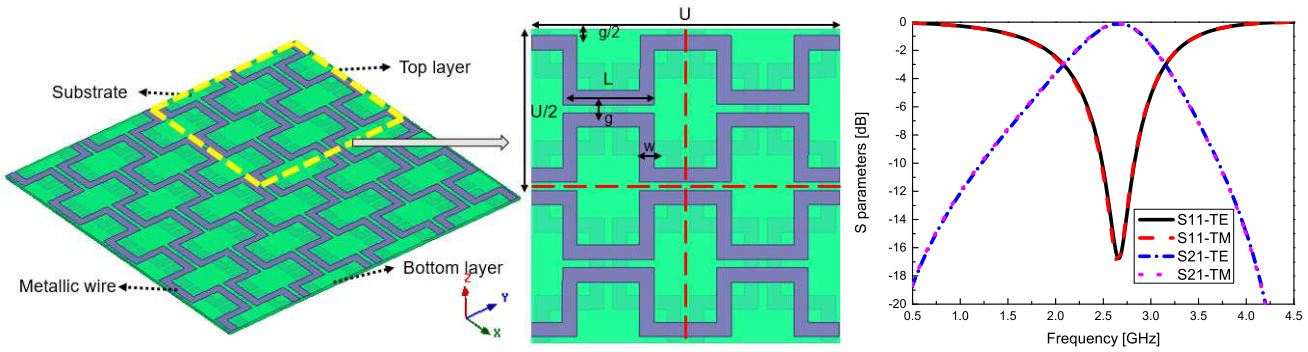

Figure 1. Dual-polarized PFSS model. (a) Three-dimensional, (b) unit cell parameters, (c) transmission and reflection coefficient under two polarizations.

2.2. Dual-Polarized Switchable AFSS Model

The PIN Diode HMSP3862 [15] from Avago Company has been used in this AFSS. This device is a series connect pair of diodes in a SOT-23 package, and the important values of this PIN are: a 3 Ω resistor for the ON state (forward bias) and a 0.15 pF capacitor with a 6000 Ω resistor in parallel for the OFF state (reversed bias). The parasitic parameters of PIN's package are ignored here because they are

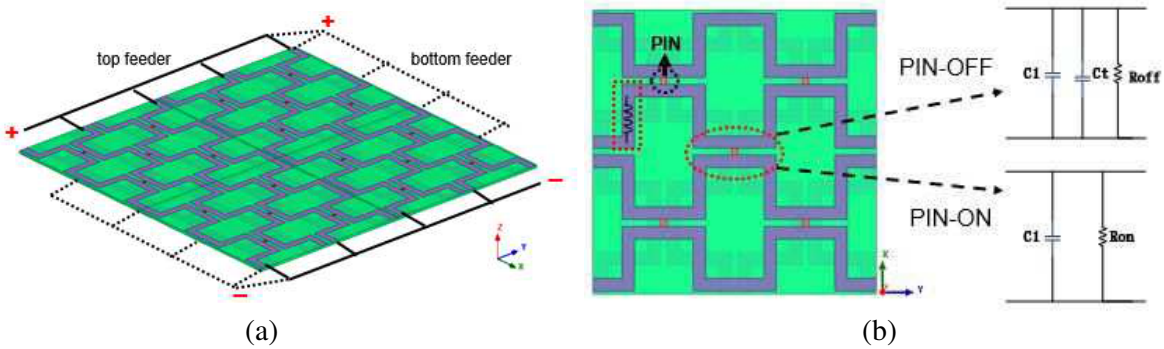

(a) (b)

Figure 2. Switchable AFSS model. (a) PIN diodes distribution and feeder topology, (b) equivalent circuit of PIN diode inside FSS.

quite small compared with the resonate parameters at concerned frequency band. The length of gap g is set as 1.5 mm, the size of PIN for welding suitably.

Figure 2 shows the PIN diodes distribution and feeder topology of the switchable AFSS model. The PINs are distributed at intervals inside the FSS elements, not each element, for saving PINs. Meanwhile, the PIN only works when the direction of electric field is parallel to connection direction, so the PINs between top and bottom layers are arranged orthogonally to overcome the polarization sensitivity. Besides, the external feeder lines on the edge of top and bottom layers are connected together to control PINs at the same time, one of which provides positive voltage, and the other provides negative voltage or ground zero voltage. This biasing network can guarantee that each PIN works and that all PINs are connected in parallel, avoiding that one bad PIN hinders the whole surface's performance. Figure 2 gives the simple equivalent circuit of the PIN [15]. When no bias is applied, the PIN will be OFF, and the Roff is quite large (e.g., 6000 Ω), which is parallel to the structure induction capacitor $C1$, so the effect of PINs is very small. However, when PIN is ON, the Ron is only 3 Ω and parallel with $C1$, so the adjacent elements are almost connected, and the whole frequency response has been changed.

2.3. Equivalent Circuit Model Analysis

Equivalent circuit model (ECM) is one useful analytical method helpful for us to understand the inside physical principle of FSS. For instance, under the normal irradiation of TE polarization (vertical polarization), the top and bottom layer structures show different induction effects shown in Figure 3. For the top layer, the direction of electrical field is vertical to meander lines, so the coupling effect $C1$ exists strongly between adjacent lines, and there is still small inductance $L1$ along the short lines. $C1$ and $L1$ are connected in series, which shows the low-pass characteristic in Figure 3(a). However, for the bottom layer, the direction of electric field is parallel to meander lines so the inductance $L2$ along the long lines are large, and the coupling effect $C2$ is small between adjoining lines. $C2$ and $L2$ are connected in parallel, which shows the high-pass characteristic in Figure 3(b). The top and bottom layers are on a thin substrate, so there is a coupling capacitance Ck between them. The whole ECM is give in Figure 3(c). The resonant frequency and variation trend are almost the same as in simulated results. The values of $C1 = 0.3$ pF, $L1 = 0.8$ nH, $C2 = 0.02$ pF, $L2 = 6$ nH and $Ck = 0.25$ pF are extracted by parameter sweeping and tuning in ADS, and $Z0 = 377\,\Omega$ is the air intrinsic impedance.

The above analysis is based on our passive FSS structure without PIN diodes. The active FSS's ECM can be obtained by adding the PIN's model into this circuit model, and this PIN model is parallel to parameter $C1$. When PINs are OFF, the large resistance $R = 6000\,\Omega$ and a RF capacitance $Ct = 0.15$ pF are parallel to $C1$ but have a little impact on the original performance, so the PIN-OFF AFSS is still band-pass, shown in Figure 4. However, if the PINs are turned ON, then R will become small only 3 Ω, and finally, the whole frequency response of PIN-ON AFSS is turned to a low level, shown in Figure 5. Through ADS simulation, the transmission results of this AFSS's ECM analysis shown in Figure 6 have realized excellent switch feature at the LTE-D 2.6 GHz band.

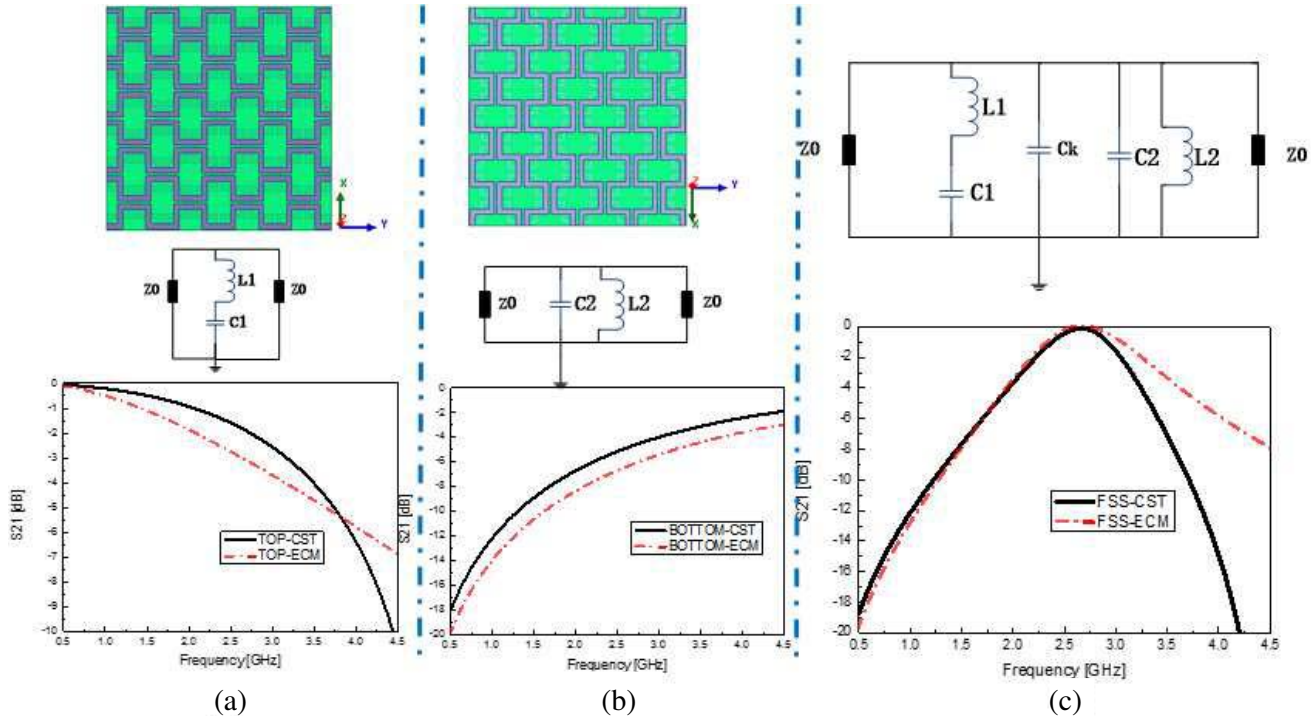

Figure 3. Equivalent circuit model of the proposed FSS, (a) the top layer, (b) the bottom layer and (c) the whole structure.

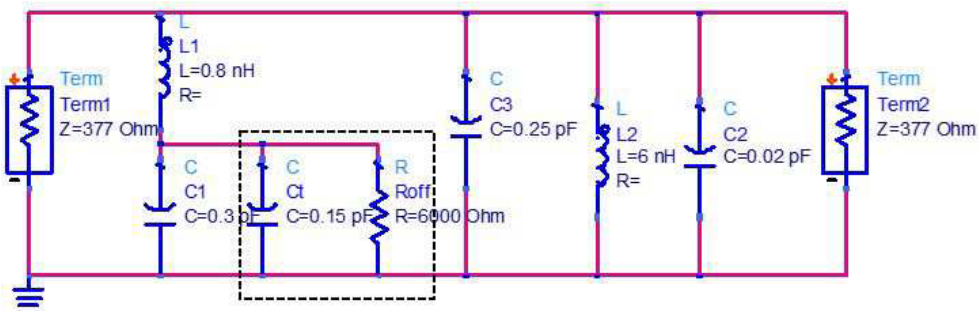

Figure 4. Equivalent circuit model of AFSS at OFF state.

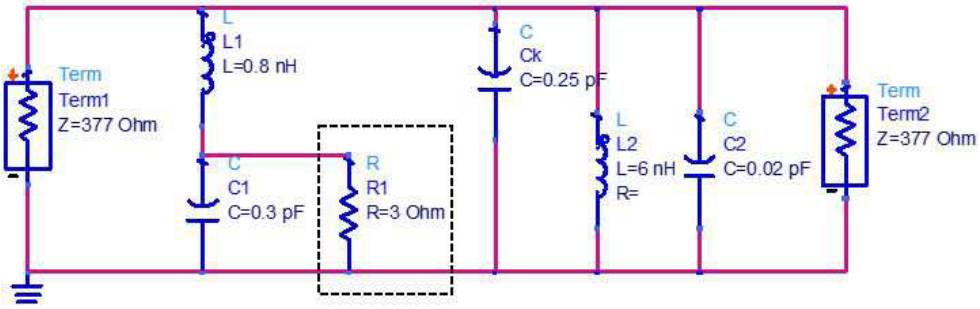

Figure 5. Equivalent circuit model of AFSS at ON state.

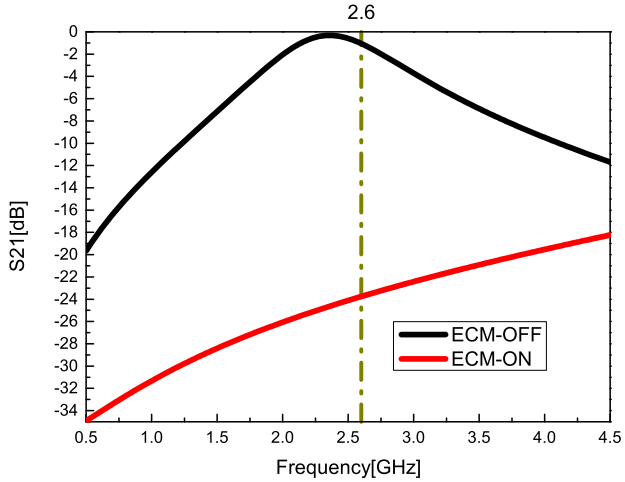

Figure 6. The ADS simulated results of equivalent circuit model of AFSS.

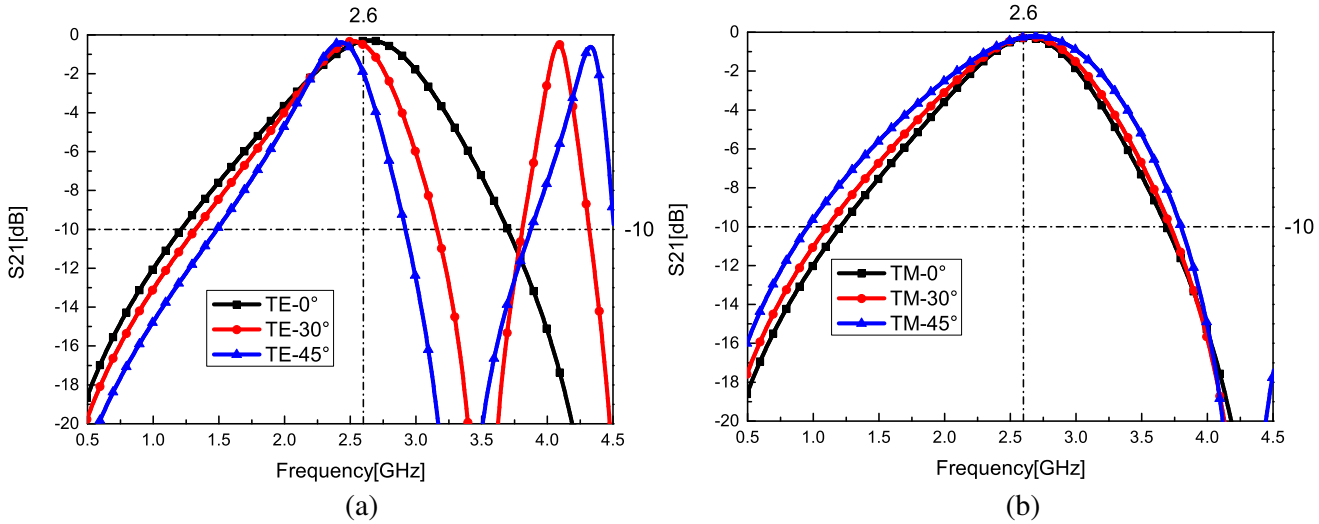

Figure 7. Transmission coefficient of OFF state under different incident angles. (a) TE polarization, (b) TM polarization.

3. STABILITY ANALYSIS

Although FSS filters can be designed to demonstrate low-pass, high-pass, band-pass or band-stop behavior as microwave filters, there is one difficulty of FSS design, i.e., the frequency response is not only the function of frequency, but also functions of incident angles of EM wave and its polarization modes.

Figure 7 and Figure 8 show the transmission coefficients of OFF and ON states under different incident angles and different polarization modes. The detailed values are list in the Table 1. When PINs are OFF, the transmission coefficients for both TE and TM are completely the same under normal incidence. The variation trends of curves with the increase of angle are opposite. For TE mode, the center frequency and -3 dB bandwidth grow smaller when the angle increases, and the grating lobes arise in advance; for TM mode, the center frequency and -3 dB bandwidth become larger when the angle increases. When PINs are ON, the whole surface should reject 2.6 GHz signals transmission. For TE mode, the reject level grows larger when the angle increases. Under 45°, the reject can be -14.2 dB. For TM mode, the rejection is weakened when the angle increases. Under 45°, the level is -7.05 dB. For the perfect applications, this design needs optimization for larger rejection in the future.

The substrate thickness will obviously affect the performance of our AFSS for the resonant

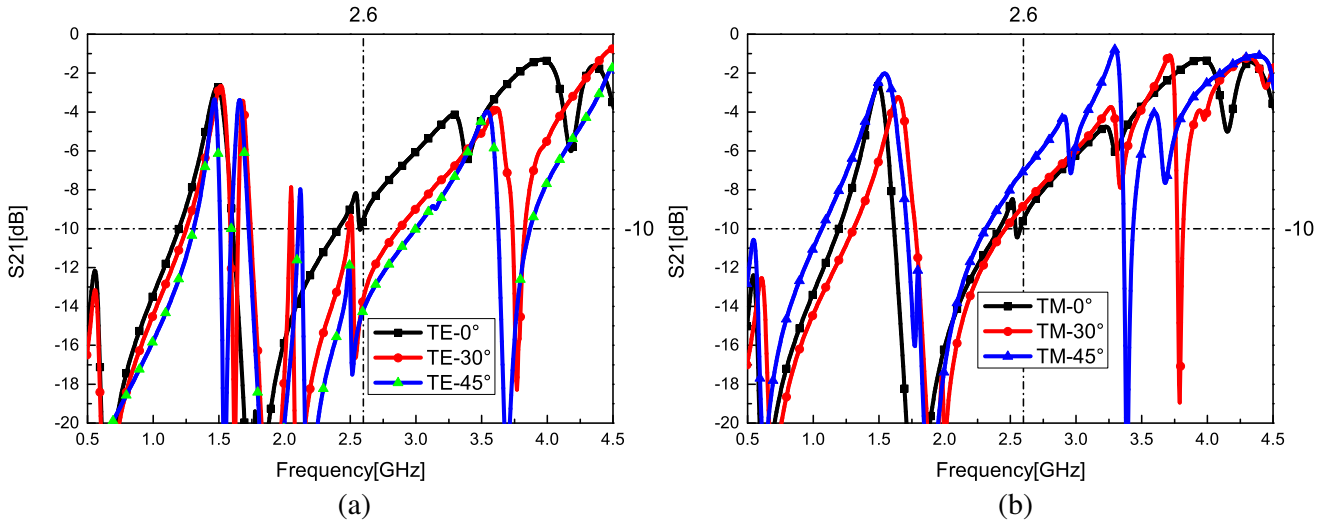

Figure 8. Transmission coefficient of ON state under different incident angles. (a) TE polarization, (b) TM polarization.

Table 1. Detailed values of the switchable AFSS.

State	Index	0°		30°		45°	
		TE	TM	TE	TM	TE	TM
OFF	Center frequency [GHz]	2.65	2.65	2.54	2.66	2.43	2.70
OFF	Insert loss @2.6 GHz [dB]	−0.3	−0.3	−0.5	−0.3	−1.9	−0.3
OFF	−3 dB bandwidth [GHz]	1.06	1.06	0.74	1.16	0.513	1.39
ON	Rejection @2.6 GHz [dB]	−9.55	−9.54	−13.6	−8.82	−14.2	−7.05

frequency, bandwidth and other parameters. If thickness changes, the coupling between two FSS layers will break, and the resonant characteristic may disappear.

4. MEASUREMENT SETUP

To further verify the preliminary results, a prototype of the double-layer coupled meander-line AFSS is fabricated and measured using the free-space measurement method. Figure 9 shows the AFSS sample with 10×10 elements on each layer and overall dimension of 320 mm × 320 mm. Common DC feeder lines (+/−) are arranged on both sides. The positive lines on the top and bottom layers are combined together, then all PINs can be controlled at the same time. The substrate is the same as that used in the simulation. The PIN diodes HSMP3862 from Avago are employed as RF switches because they have low resistance when forward biased and cheap price. The amount of PINs used in this sample is 290, which is bearable within the manufacturing cost range.

The measurement is carried out in a microwave anechoic chamber using two horn antennas (0.8–6 GHz) system, one for transmitting signals and the other for receiving signals, and these two antennas connected by an Agilent N5230C vector network analyzer (VNA) in Figure 9. Considering the problem of background noise and normalization, two steps for the calibration are necessarily implemented. Firstly, the transmission coefficients $T0$ (in dB) are measured without FSS; then the transmission coefficients $T1$ (in dB) are measured with FSS and other things unchanged. In the end, the transmission characteristic T (in dB) of FSS can be calculated by $T = T1 - T0$.

A DC stabilized voltage source is used to provide bias onto the AFSS. With no voltage, PIN diodes are at OFF state. When the voltage is 3.3 V, the diodes are turned ON. It should be noted that the voltage must be lower than the voltage limitation. Otherwise, the PINs will be destroyed. The

simulated and measured results under normal incidence of two states have been compared and plotted in Figure 10. For both OFF and ON states, the center frequency, isolation level at 2.6 GHz and variation trend coincide well. The transmission characteristics of the proposed structure under oblique incidence angles are depicted in Figure 11 and display good stability for large incident angles up to 45°. The large

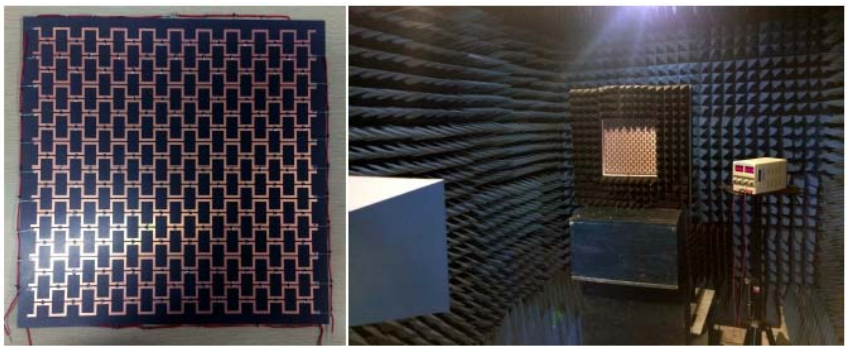

Figure 9. The switchable AFSS prototype with PINs and external feeders and the transmission measurement setup showing that the AFSS fixed in a bracket between two horn antennas system.

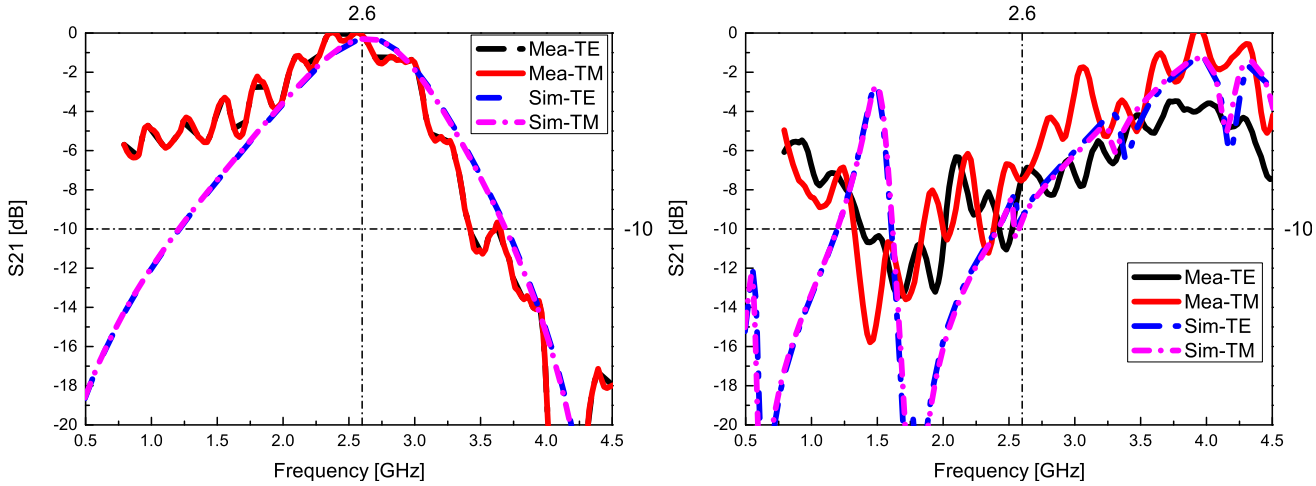

Figure 10. Measured and simulated S_{21} results under PIN-OFF and PIN-ON states for TE and TM polarizations.

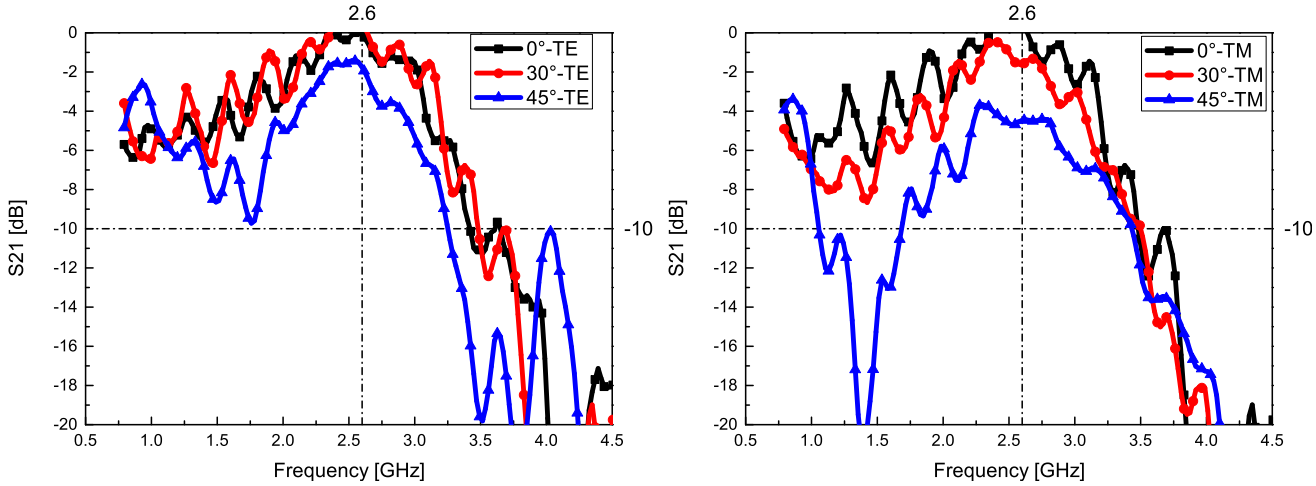

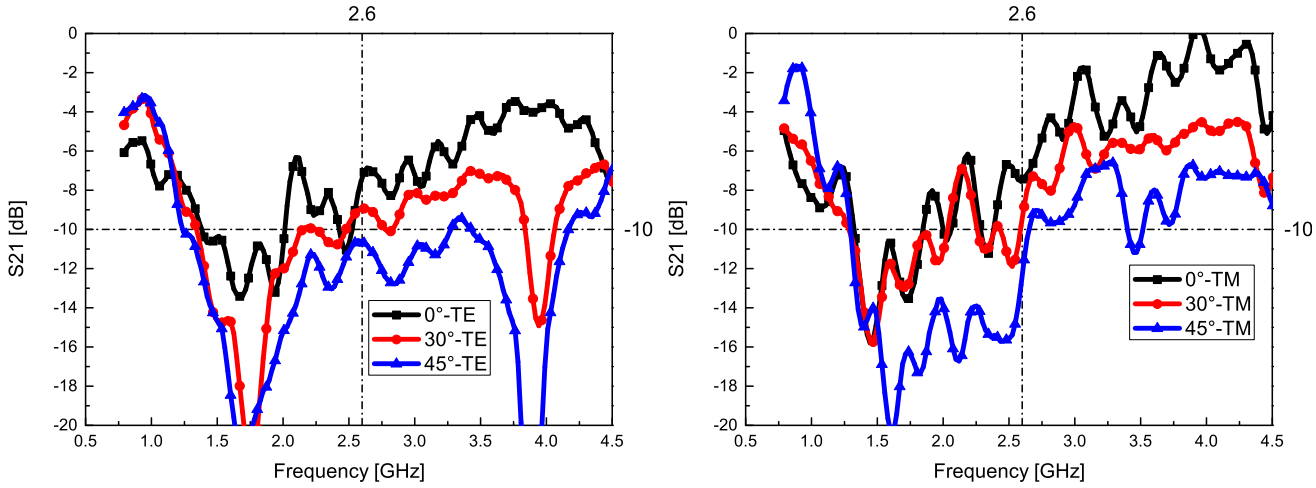

Figure 11. Measured S_{21} results at different incident angles.

insert loss at OFF state of 45° could be contributed to the limited bracket made of absorptive material and the horn antennas with large aperture, which can be avoided by using larger AFSS surface and better measurement equipment.

5. CONCLUSION

In this paper, a new dual-polarized AFSS filter with switchable function at LTE-D band 2.6 GHz is proposed, designed, fabricated and measured using coplanar resonant feed array and appropriate amount of active device PIN diodes. According to both simulated and measured results, the isolation between ON-state and OFF-state at 2.6 GHz is almost 10 dB, which can be enlarged in the future research. The ECM analysis is used for intensive understanding. The transmission coefficient keeps a good stability under different incident angles till 45° and different polarizations (TE/TM) for working in the complex EM environment. This design has potential applications in intelligent EMC, stealth radome, smart buildings and so on.

ACKNOWLEDGMENT

This work is supported by the Jiangsu Industry-University-Research Cooperation Innovation Project under grant BY2014003-10, Nanjing Industry-University-Research Cooperation Innovation Project under grant No. NBG0030113-1 and National Natural Science Foundation of China under grant No. 61401199.

REFERENCES

1. Unal, E., A. Gokcen, and Y. Kutlu, "Effective electromagnetic shielding," *IEEE Microwave Magazine*, Vol. 7, No. 2, 48–54, 2006.
2. Munk, B. A., *Frequency Selective Surfaces: Theory and Design*, Wiley, New York, USA, 2005.
3. Chang, T. K., R. J. Langley, and E. A. Parler, "An active square loop frequency selective surface," *IEEE Microw. Guided Wave Lett.*, Vol. 3, No. 10, 387–388, 1993.
4. Chang, T. K., R. J. Langle, and E. A. Parker, "Active frequency selective surface," *IEEE Proc., Part H*, Vol. 143, 62–66, 1996.
5. Kiani, G. I., K. L. Ford, K. P. Esselle, and A. R. Weily, "Oblique incidence performance of an active square loop frequency selective surface," *The 2nd Eur. Conf. on Antennas and Propag.*, Edingurgh, U.K., Nov. 11–16, 2006.

6. Kiani, G. I., K. L. Ford, L. G. Olsson, K. P. Esselle, and C. J. Panagamuwa, "Switchable frequency selective surface for reconfigurable electromagnetic architecture buildings," *IEEE Trans. Antennas Propag.*, Vol. 58, No. 2, 581–584, 2010.
7. Taylor, P. S., E. A. Parker, and J. C. Batchelor, "An active annular ring frequency selective surface," *IEEE Trans. Antennas Propag.*, Vol. 59, No. 2, 3265–3271, 2011.
8. Yang, C., H. Li, Q. Cao, and Y. Wang, "Switchable electromagnetic shield by active frequency selective surface for LTE-2.1 GHz," *Microwave and Optical Technology Letters*, Vol. 58, No. 3, 535–540, 2016.
9. Mias, C., "Frequency selective surfaces loaded with surface-mount reactive components," *Electron. Lett.*, Vol. 39, No. 9, 724–726, 2003.
10. Mias, C., "Waveguide and free-space demonstration of tunable frequency selective surface," *Electron. Lett.*, Vol. 39, No. 14, 1060–1062, 2003.
11. Sanz-Izquierdo, B., E. A. Parker, and J. C. Batchelor, "Dual-band tunable screen using complementary split ring resonators," *IEEE Trans. Antennas Propag.*, Vol. 58, No. 11, 3761–3765, 2010.
12. Che, Y. X., X. Hou, and Z. Gao, "A tunable miniaturized-element frequency selective surfaces without bias network," *IEEE International Conference of Microwave Technology and Computational Electromagnetics (ICMTCE)*, 70–73, 2011.
13. Xu, X. H., Y. Zhao, and F. C. Yu, "A novel horizontal polarization sensitive active frequency selective surface without biasing network at 2.4 GHz WiFi band," *IEEE 3rd Asia-Pacific Conference of Antennas and Propagation (APCAP)*, 2014.
14. Sanz-Izquierdo, B. and E. A. Parker, "Dual polarized reconfigurable frequency selective surfaces," *IEEE Trans. Antennas Propag.*, Vol. 62, No. 2, 761–771, 2014.
15. [Online], available: http://www.avagotech.com/docs/AV02-0293EN.